17th World Conference on Earthquake Engineering, 17WCEE

Sendai, Japan - September 13th to 18th 2020

LESSONS LEARNT FROM BUILDINGS DAMAGED IN THE 2018 HUALIEN EARTHQUAKE, TAIWAN

Y. H. Tu[(1)], T. Yeh[(2)]

[(1)] *Professor, Department of Architecture, National Cheng Kung University, yhtu@mail.ncku.edu.tw*
[(2)] *Master of Science, Department of Architecture, National Cheng Kung University, tim41601@yahoo.com.tw*

Abstract

The Hualien earthquake, which had a Richter magnitude scale of 6.26, occurred on February 6, 2018. Among the buildings reported damaged, all four buildings that collapsed were higher than six stories. This was ascribed to the effect of near-fault ground motions since most of the damaged buildings were located along the Milun Fault. The authors investigated the damage to 13 buildings within one week after the earthquake. The observations included buildings located close to each other that showed different degrees of damage. The structural information was acquired from an on-site survey and from architectural blueprints that were collected afterward. The ground motion intensity at each building site was estimated using linear interpolation from the peak ground accelerations recorded by nearby seismic stations. This paper presents the results of the reconnaissance and discusses the possible reasons behind the concentration of damage in the higher buildings.

A medium positive correlation was found between the damage state and the number of stories in the investigated buildings. The response spectra plotted from the ground motion records of multiple stations in Hualien City also showed higher spectral accelerations in the approximate period range corresponding with the severely damaged buildings. However, the height of building was not solely responsible for the earthquake damage that it experienced. It was found that the buildings with a higher ratio of column area and wall area to the total floor area tended to have less damage. The relationship between the building age and the damage state was not clear, but none of the damaged buildings were built after the major modification of the seismic design regulations in 1997. In addition to the factors the buildings had in common, specific flaws may have aggravated the level of damage. Two older commercial buildings with damage histories in former earthquakes were claimed to have been retrofitted but were found to be seriously damaged or collapsed in this earthquake. Construction defects and illegal renovations were found in three collapsed residential buildings although it was difficult to verify the connections between the defects and the damage.

Other than the 13 buildings under consideration, the authors also visited several elementary schools. After past earthquakes, typical school buildings in Taiwan were found to be vulnerable to earthquake damage. Therefore, the school buildings in Hualien City had been retrofitted with RC shear walls, side-walls, and RC column jacketing. These retrofits proved to be effective and only slight damage to non-structural elements were found.

Keywords: Building; Damage; Reconnaissance; Reinforced Concrete

1. Introduction

The rapid collision between the Eurasia and Philippine Sea Plates causes frequent seismic activities along the Longitudinal Valley in eastern Taiwan. The Hualien area in the northern Longitudinal Valley is one of the highest seismic zones in Taiwan. The 2018 Hualien earthquake occurred on February 6 at 23:50 local time. The Richter magnitude scale was 6.26 and the moment magnitude (M_w) was 6.4. The epicenter was located at 24.10◦N, 121.73◦E offshore of the city of Hualien. The focal depth was 6.31 km. The maximum observed peak ground acceleration (PGA) and peak ground velocity (PGV) at various stations were 5.94 m/s^2 and 1.46 m/s, respectively. In the Hualien City area where the most damage was reported, the maximum observed PGA was 4.03 m/s^2 or 0.411 g. The reported damage included one severely damaged building, four collapsed buildings, upheaval of bridge decks, and damage to non-structural components in hospitals [1]. 14 of the earthquake's 17 fatalities died in one of the collapsed buildings.

The authors arrived in Hualien City and started a three-day reconnaissance on February 8, 2018. We investigated the damage to 13 buildings in the Hualien downtown area, including the severely damaged and collapsed buildings and the buildings located close to those buildings. Because all four buildings that collapsed were higher than six stories, the main purpose of the reconnaissance was to study the possible reasons behind the concentration of damage in the higher buildings. We also visited three elementary schools that have been retrofitted before the earthquake to study the effect of their seismic retrofitting. Structural information such as the plan layouts of 12 of the 13 buildings was acquired from the on-site survey and from architectural blueprints that were collected afterward. The ground motion intensity at each building site was estimated using linear interpolation from the PGAs recorded by nearby seismic stations. This paper presents the results of this reconnaissance and discusses the relationships between the building damage and structural and ground motion factors.

2. Site and Building Information

2.1 The seismic event

More than one research study has suggested that the 2018 Hualien earthquake was induced by multiple faults. Huang & Huang's analysis [2] showed that at least three faults were involved in the event, including a south-dipping fault, a main west-dipping fault, and the east-dipping Milun fault located in Hualien City. Lo et al. [3] proposed that the dynamic rupture process occurred on the offshore inter-plate fault, the Meilun fault and the Longitudinal Valley fault. Dynamic slips were partitioned as thrust and strike-slip motions on the offshore fault and the Meilun fault, respectively. The Central Geological Survey (CGS) in Taiwan found obvious left-lateral slips along the Milun and Lingding faults after the earthquake [4]. The area east of the faults has been uplifted over time to form the Meilun tableland. The tableland was found uplifted more than 40 cm and moved northeast about 50 cm during this earthquake, while the area west of the faults showed southward motion [5]. Yen et al. [5] proposed that the two faults are linked strands in the same fault zone because they slipped in similar fashion.

2.2 The site condition and ground motions

The Central Weather Bureau in Taiwan has installed more than 800 free-field strong motion stations throughout Taiwan. The ground motion data of this event is available via the geophysical database management system (GDMS) [6]. Kuo et al. [7] plotted the S-wave velocity (V_{S30}) map using the V_S profiles logged at most of the free-field strong-motion stations [8]. The map showed that the V_{S30} in the Hualien area was mostly between 360 and 760 m/s and belonged to site class C; part of Hualien City was site class D with a V_{S30} between 240 and 360 m/s. Kuo et al. [7] also analyzed the microtremor horizontal-to-vertical spectral ratio in the Hualien area. They found that the predominant frequencies that occurred in downtown Hualien were 0.8–1.5 Hz and changed to 1.2–1.5 Hz to the west.

Kuo et al. [7] reported that typical near-fault strong ground motions with pulse-like velocities were recorded during the mainshock at all stations on both sides of the Milun fault within 4 km. The maximum pulses were mostly in the fault-normal direction (east–west). Near-fault ground motions with large amplitude and long-period pulses are believed to be destructive for medium- to high-rise buildings [9]. Kuo et al. [7] compared the spectral accelerations of 17 stations that showed velocity pulses with the design spectrum for this region. The comparison showed that spectral accelerations at periods longer than 1.5 s exceeded the design spectrum. Kuo et al. [7] also found that the closest stations to the collapsed medium rise buildings recorded an obvious spectral acceleration peak of roughly 1 s from the north–south component and another peak of approximately 2 s from the east–west component. They suggested that the strong shaking during the period of 1 s may have been the major cause of the collapse of the four medium-rise buildings.

2.3 The investigated buildings

Thirteen buildings were heavily damaged in the earthquake, including three low-rise street-houses, four mid-rise residential buildings, one low-rise commercial building, two mid-rise commercial buildings, and two mid-rise complex buildings. All thirteen buildings except building D were reinforced concrete (RC) buildings. Building D was a confined masonry (CM) building with RC frames and masonry walls made of clay bricks. Table 1 summarizes the information about the buildings. The damage state of each building was determined in accordance with a five-level procedure [10]. The levels I, II, III, IV, V and V+ represent slight, light, moderate, severe, total damage and collapse, respectively. Fig. 1(a) shows the locations of the thirteen buildings and the Milun fault. Among the four buildings that collapsed, three (I, K, M) were within 200 m of the fault. All thirteen buildings, except for one (H) were within 500 m of the fault. The PGA at each building site was estimated using linear interpolation from the strong motions recorded by nearby seismic stations, as shown in Fig. 1(b). Table 2 shows the PGAs in the north-south (NS), east-west (EW) and vertical (UD) directions recorded by the seismic stations. Because the buildings did not necessarily lie in a NS or EW direction, the interpolated PGA along the plan direction of each building was obtained by adding a coordinate rotation to the original strong motion records. The shaded areas in Table 1 mark the larger PGAs along two orthogonal plan directions. The differences between the PGAs of buildings are not large and seem not to be proportional to the damage states.

Table 1 – Summary of the investigated buildings

Building	Type	No. of stories	Basement	Height (m)	Age	Damage state	PGA along the plan direction	
							X-dir. (gal)	Y-dir. (gal)
A	Commercial	8	1	25.9	36	I	260.8	307.0
B	Street-house	4	-	13.5	43	II	269.3	223.8
C	Residential	6	1	18.9	24	III	228.2	264.1
D	Street-house	3	-	9.4	57	I	228.2	260.7
E	Residential	6	-	21.2	28	II	213.9	264.8
F	Street-house	5	1	16.5	25*	I	293.3	234.6
G	Complex	12	2	41.3	21	I	291.6	247.5
H	Commercial	3	-	11.9	30	III	222.7	191.8
I	Residential	6	1	25.3	25*	V+	258.3	226.2
J	Complex	12	1	35.9	24	V+	235.0	293.5
K	Commercial	11	1	32.0	41	V+	261.8	314.1
L	Commercial	11	2	36.5	39	IV	199.9	206.5
M	Residential	9	-	30.5	25*	V+	259.1	226.6

*: Estimated age

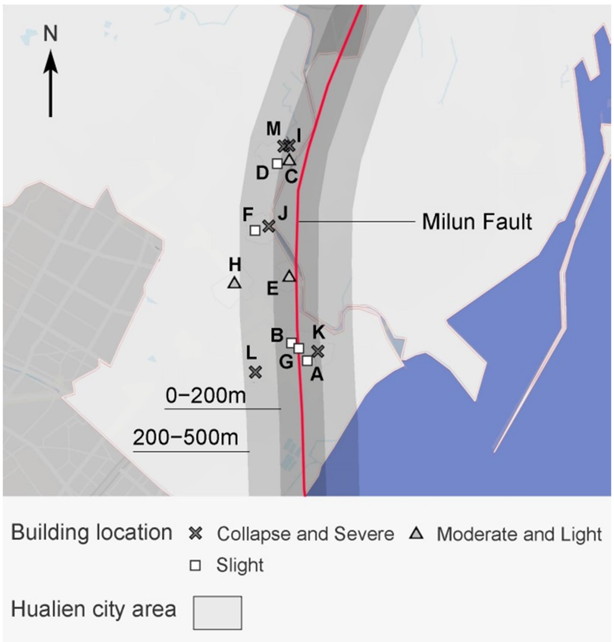

(a) Distance from the fault to the buildings

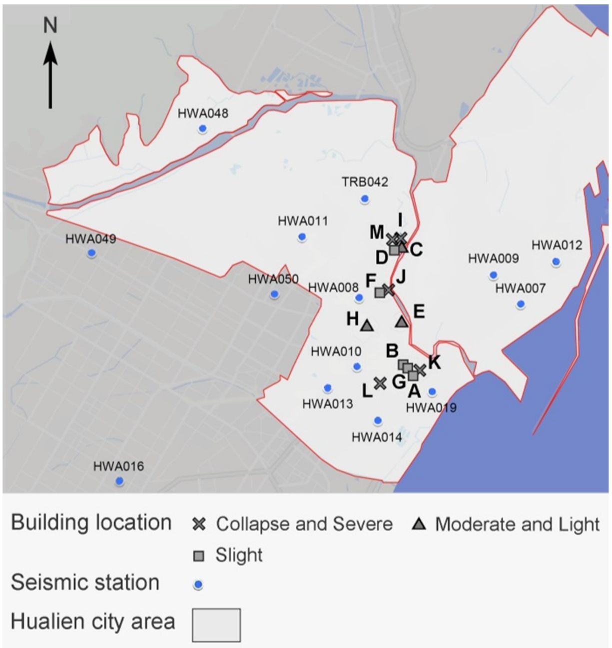

(b) The 14 seismic stations used for interpolation

Fig. 1 – Locations of the investigated buildings and seismic stations

Table 2 – Summary of the investigated buildings

Station	Longitude	Latitude	PGA-NS (gal)	PGA-EW (gal)	PGA-UD (gal)
HWA012	121.6313	23.9920	280.62	279.70	338.37
HWA007	121.6262	23.9865	244.20	289.02	259.95
HWA009	121.6223	23.9903	262.02	249.88	317.55
HWA019	121.6135	23.9750	370.24	403.30	213.44
HWA014	121.6057	23.9712	218.82	316.99	397.08
TRB042	121.6038	24.0003	188.88	204.35	219.17
HWA008	121.6030	23.9873	336.48	230.23	330.81
HWA010	121.6027	23.9783	78.62	62.10	93.72
HWA013	121.5985	23.9755	149.13	65.10	144.40
HWA011	121.5948	23.9953	199.21	247.94	327.11
HWA050	121.5908	23.9878	198.21	279.04	336.94
HWA048	121.5805	24.0095	303.27	204.56	271.35
HWA016	121.5685	23.9632	161.21	198.54	258.66
HWA049	121.5645	23.9932	240.62	316.80	262.77

Fig. 1(a) shows that some buildings are located very close to each other, because the authors purposely chose to inspect the buildings in the vicinities of the four collapsed buildings for comparison. Fig. 2 shows three enlarged area plans around the collapsed buildings, including the Marshal Hotel (K), the Yunmen-Tzueti complex building (J), the Baijin-Shuangxing apartment (I) and the Wuju-Wusu apartment (M).

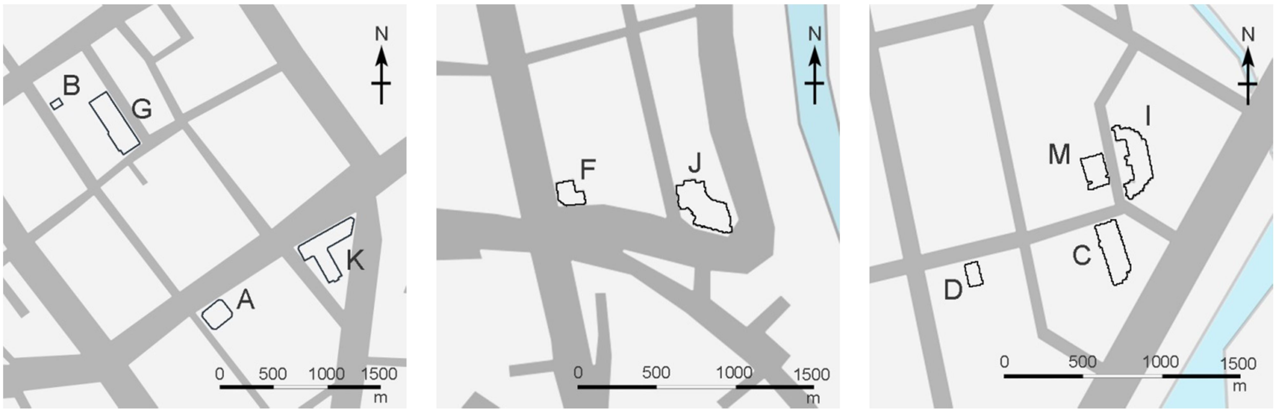

(a) Marshal Hotel area (b) Yunmen complex area (c) Kuoshen 6 Street area

Fig. 2 – Enlarged area plans around the collapsed buildings

The structural information of all thirteen buildings except building M was acquired from the on-site survey and from architectural blueprints that were collected afterward. The structural plan of the ground floor and at least one upper floor of each building were redrawn by Yeh [11]. Fig. 3 shows two examples.

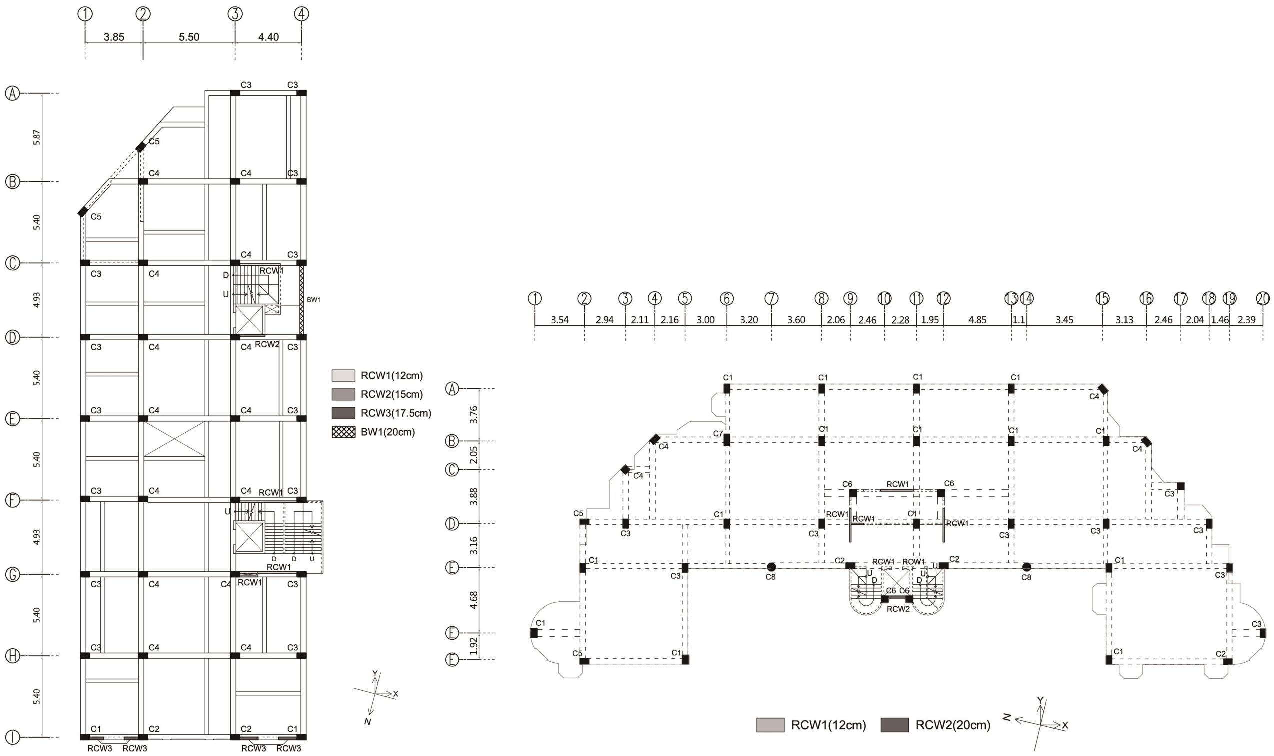

(a) Building C (b) Building I

Fig. 3 – Structural plans of the ground floors of two example buildings

Column areas and wall areas on the ground floors were calculated from the structural plans. Table 3 shows the column area ratios and the weighted wall area ratios calculated by dividing the column areas and the weighted wall area by the floor areas above the first floor, respectively. The weighted wall area was obtained by summing the areas of RC walls that have four sides, three sides, two sides attached to the frames and the masonry walls that have four sides and three sides of confinement multiplied by a weighting factor of 1.0, 0.67, 0.33, 0.2, and 0.067, respectively. The weighting factors were determined in accordance with the shear strength per unit area suggested by JBDPA [12] and Lu [13] for the different types of walls, as shown in Table 4. The shear strengths per unit area of RC columns with a slenderness ratio smaller and larger than 6.0 were 0.980 MPa and 0.686 MPa, respectively, as suggested by JBDPA [12]. In order to reflect the composite effect of columns and walls on their lateral resistance, a vertical member area ratio was obtained from the summation of the column area and the wall area transformed in accordance with the proportion of shear strengths of walls to columns. That means the weighted wall area ratios in Table 3 were multiplied by 2.940/0.980=3.0 and added to the column area ratios to obtain the vertical member area ratios. The column area ratios of buildings B, D, E, F, H, and I in Table 3 were multiplied by 0.686/0.980=0.7 before the summation, because most of their columns at GF had a slenderness ratio larger than 6.0.

Table 3 – Column area ratios of the investigated buildings

Building	Floor areas above the first floor (m^2)	Column areas at GF (cm^2)	Column area ratio (cm^2/m^2)	Weighted wall area ratio (cm^2/m^2)		Vertical member area ratio (cm^2/m^2)	
				X-dir.	Y-dir.	X-dir.	Y-dir.
A	3729.0	100800	27.03	20.20	11.04	87.62	60.14
B	258.8	13000	50.23	16.23	41.04	83.85	158.27
C	2749.9	73500	26.73	6.90	0.00	47.44	26.73
D	304.5	11340	37.24	6.73	25.02	46.25	101.12
E	1799.6	49800	27.67	6.72	0.00	39.53	19.37
F	1057.3	34900	33.00	15.41	34.84	69.33	127.62
G	8750.6	252700	28.87	6.62	9.05	48.75	56.04
H	429.6	23350	54.35	0.00	0.00	38.05	38.05
I	3554.3	114200	32.13	1.07	0.54	25.69	24.10
J	9209.6	204200	22.17	4.02	3.77	34.23	32.62
K	13499.7	262400	19.44	7.39	2.72	41.61	27.59
L	11102.5	191300	17.23	2.63	2.79	25.12	25.61
M	-	-	-	-	-	-	-

Table 4 – Shear strength of different types of walls

Confining condition	Shear strength per unit area (MPa)	
	RC walls	Masonry walls
Four-sides	2.940	0.588
Three-sides	1.960	0.196
Two-sides	0.980	0

3. Discussion on the Possible Reasons for Building Damages

3.1 The building age

The Seismic Building Codes in Taiwan had been majorly revised three times in 1974, 1982, and 1997, respectively. Fig. 4(a) shows the relationship between the years of construction and the damage states of the thirteen buildings, with the exception of buildings F, I, and M because their exact years of construction were not available. Although the older buildings are believed to have lower seismic resistance, the figure shows no clear relationship between the damage and the age of a building. A possible reason is that most of the old buildings might have been damaged during past earthquakes and demolished or renovated, since the Hualien area has frequent seismic activities. Fig. 4(a) also shows that none of the damaged building was build after 1997. That means the latest major revision of the Building Codes in 1997 is efficient in seismic resistance.

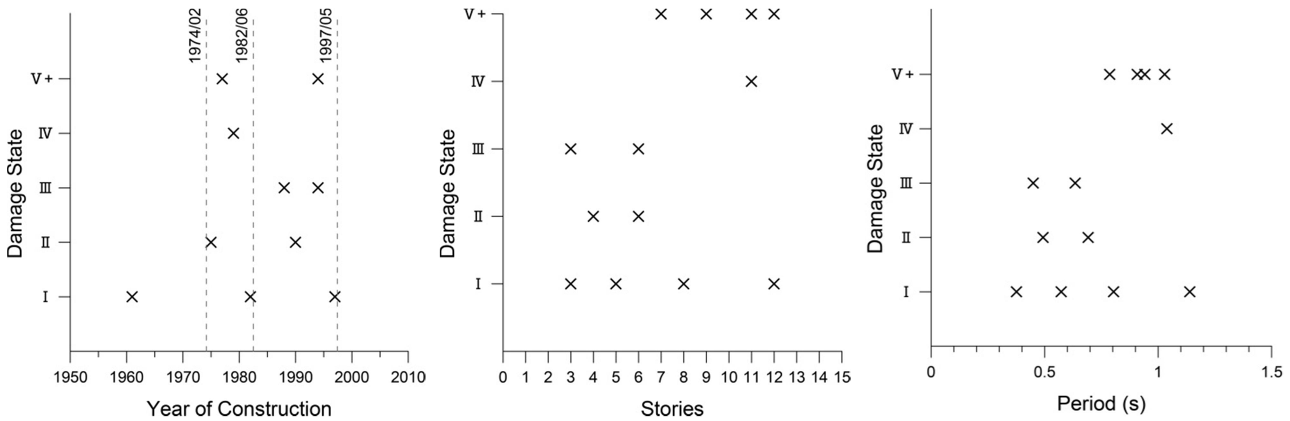

(a) Year of construction (b) Number of stories (c) Fundamental period

Fig. 4 – The relationships between the damage states and the building parameters

3.2 The building height

The four collapsed buildings (I, J, K, M) were all higher than six stories and three (J, K, M) of them were about ten-stories high. Therefore, many believe that building height was the main reason responsible for the severe damage, as suggested by Kuo et al. [7]. In order to further study the effect of the building height, the authors included four buildings (A, C, E, G) that were higher than six stories and close to the fault or to other collapsed buildings in the investigation. Fig. 4(b) shows the relationship between the numbers of stories and the damage states of the thirteen buildings. Fig. 4(c) shows the relationship between the fundamental periods and the damage states. The fundamental period T was calculated by the empirical equation suggested by the current Seismic Building Codes in Taiwan, as shown in Eq. (1). The building height h_n was substituted by the values listed in Table 1. The Pearson product-moment correlation coefficients or the R-values calculated using Eq. (2) from Fig. 4(b) and 4(c) were 0.37 and 0.43, respectively. Both values showed a medium positive correlation between the building height and the damage state.

$$T = 0.07{h_n}^{0.75} \tag{1}$$

$$R = \frac{\sum_{i=1}^{n}(x_i - \bar{x})(y_i - \bar{y})}{\sqrt{\sum_{i=1}^{n}(x_i - \bar{x})^2 \cdot \sum_{i=1}^{n}(y_i - \bar{y})^2}} \tag{2}$$

Fig. 4(c) shows that most of the collapsed and severely damaged buildings had a fundamental period close to 1.0 s. The acceleration spectra of the strong motions recorded by the four closest stations to the buildings were compared with the design spectra, as shown in Fig. 5. In opposition to the design spectra showing a platform for the period between 0.150–0.751 s, most of the recorded spectra showed large spectral acceleration (S_a) for the period higher than 0.751 s. Fig. 5 shows that the NS and EW spectra of HWA014 had a common peak value at about 0.85 s. The NS and EW spectra of HWA019 showed peak values of about 0.75 s and 1.05 s, respectively. The EW spectrum of TRB042 showed a peak of about 1.1 s. These periods corresponded with the fundamental periods of the collapsed and severely damaged buildings plotted at the top of the figures. They also corresponded with predominant frequencies (0.8–1.5 Hz) in downtown Hualien as reported by Kuo et al. [7]. However, both Fig. 4 and Fig. 5 show that there were also buildings (A & G) in the period region that had only slight damage. Therefore, the building height may be a major reason but not the only factor affecting the building damage.

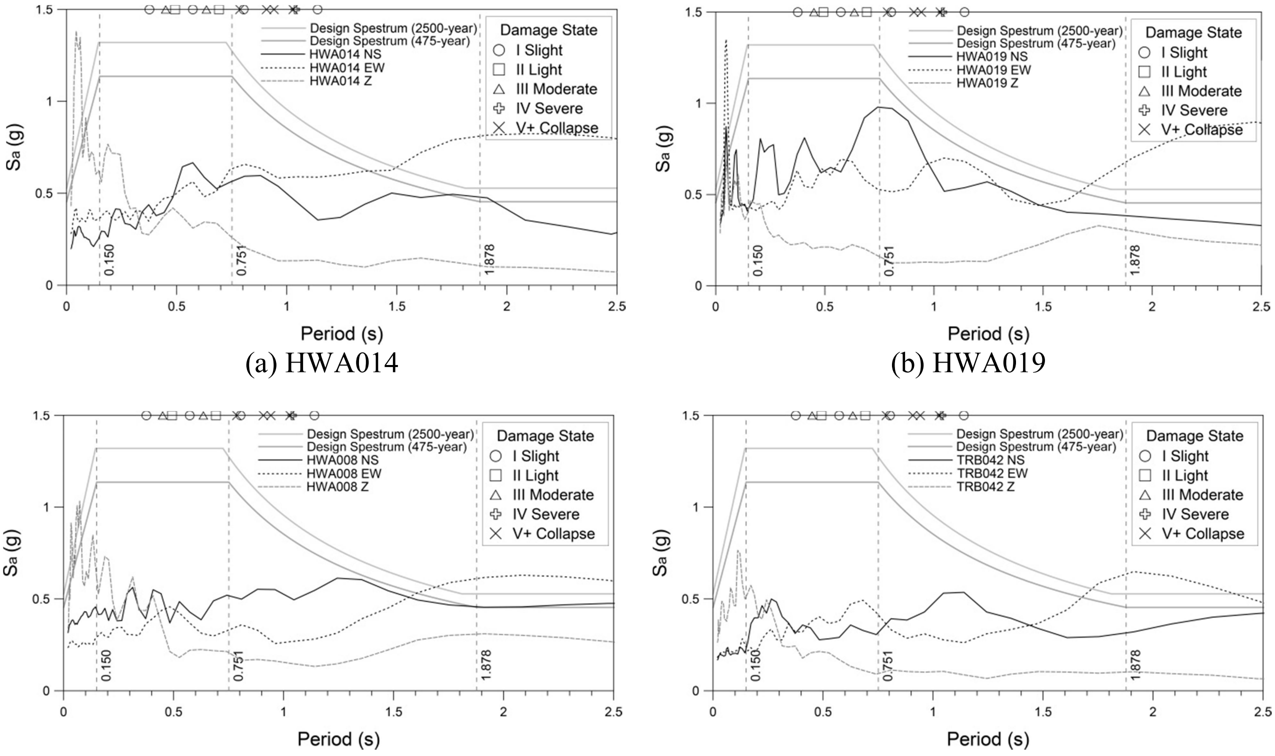

(a) HWA014 (b) HWA019

(c) HWA008 (d) TRB042

Fig. 5 – The comparisons between the recorded spectra and the design spectra

3.3 The column and wall areas

Section areas of the vertical members including the columns and walls in the ground floors are commonly used [12][14] as indexes to rapidly evaluate the seismic resistance of RC buildings. Fig. 6 shows the relationships between the damage states and the vertical member area ratios as well as the wall area ratios in the weak direction. The weak direction was determined by the lesser between the values in the X-dir. and the Y-dir., as listed in Table 3.

Fig. 6(a) shows that the damage state tended to decrease when the vertical member area ratio increased. The R-value calculated from this figure was −0.63, meaning a high negative correlation. Fig. 6(b) shows the distributions of vertical member area ratio and weighted wall area ratio with the damage state of each building represented by different signs. The signs lying on the vertical axis represent the buildings had no wall in their weak direction. This figure shows that all the collapsed and severely damaged buildings had a vertical member area ratio lower than 40 cm^2/m^2 and a weighted wall area ratio lower than 5 cm^2/m^2. In contrast, all the buildings that had a vertical member area ratio higher than 40 cm^2/m^2 and a weighted wall area ratio higher than 5 cm^2/m^2 also had only light or slight damage. The buildings A and G discussed earlier are marked in Figs. 6(a) and 6(b). The high vertical member area and wall area ratios might be the reason that they performed better than the other buildings that had similar heights. Although some may debate that the vertical member area can not reflect the effect of reinforcement, such as the hoops related to ductile or non-ductile design, these figures indicate that the column and wall areas obviously affect seismic resistance.

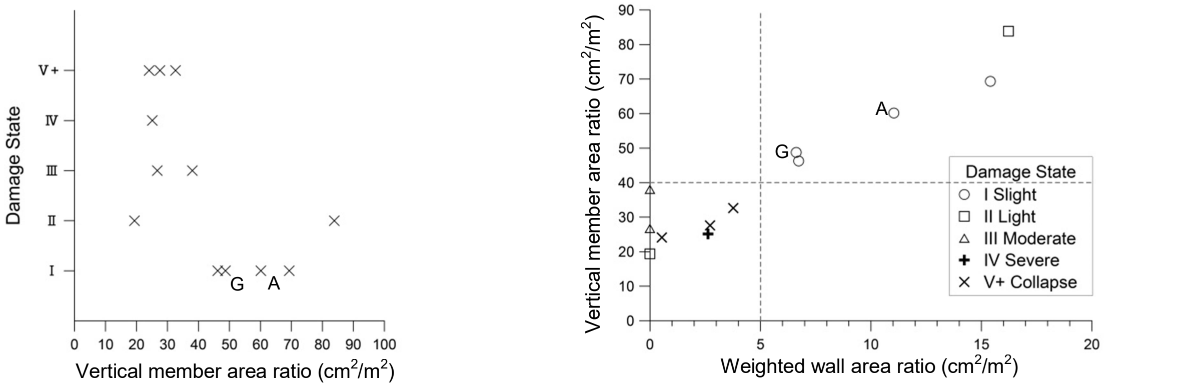

(a) Damage state vs. vertical member ratio (b) Distributions of vertical member and wall area ratios

Fig. 6 – The relationships between the damage states and the vertical member areas

3.4 Other factors

Besides the factors discussed above, specific flaws may have aggravated the damage in the collapsed and severely damaged buildings (I, J, K, L, M). The condition of each building is discussed below.

3.4.1 Marshal Hotel (Building K)

The picture of the damaged Marshal Hotel showed a typical soft/weak-base-floor failure pattern as shown in Fig. 7(a). It was obviously caused by the ground lobby floor that had few walls and upper guestroom floors with a lot of partition walls made of RC and masonry, as shown in Figs. 7(b) and 7(c). Pictures of the hotel before the earthquake showing steel members attaching to the veranda at the ground floor can be found on Google Street-view. It was rumored that the steel members were used as part of a seismic retrofit. However, they were found severely distorted after the earthquake and were obviously inefficient in resisting lateral load. There were signs indicating that the hotel had been renovated and a new façade had been added. It is possible that the earthquake inertial force was increased due to the additional weight of the added materials.

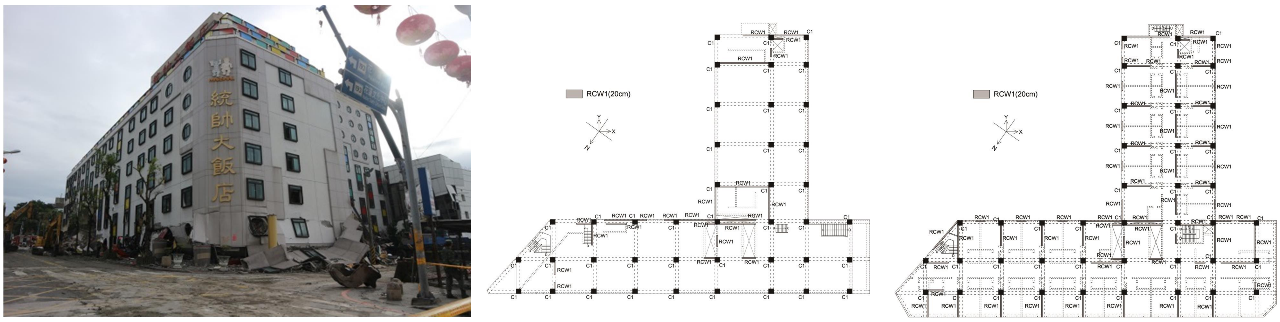

(a) Picture after the earthquake (b) Structural plan of GF (c) Structural plan of 2F

Fig. 7 – The picture and structural plans of Marshal Hotel

3.4.2 The old Far East department store (Building L)

The building was subjected to moderate damage during the 1999 Chi-Chi earthquake. Although it had been retrofitted after the 1999 earthquake, the columns at the GF facing the street all failed by shear force during the 2018 earthquake, as shown in Fig. 8(a). Hoops at a spacing of 200 – 250 mm were found fractured as shown in Fig. 8(b). The non-ductile design was obviously responsible for the shear failure of the columns. Fig. 8(c) shows that the steel braces installed for retrofit stopped at the second floor instead of continuing to the foundation for some unknown reason. The insufficiency of the retrofit might be the reason that the building was damaged again.

(a) Shear failure of the columns (b) Fractured hoops (c) Retrofit members

Fig. 8 – The pictures of the old Far East department store

3.4.3 Yunmen-Tzueti complex building (Building J)

There was a lot of speculation about the reason for the collapse of this building that caused 14 fatalities. The first speculation was that the damage was due to the soft-base-floor effect because it was a complex building with a restaurant at the GF and residential upper floors. A lot of masonry partition walls were added to the second floor when this floor was renovated to be a hotel. However, the collapsed floors included not only the soft GF, but also the B1F, 1F/GF, 2F, and 3F. Construction flaws have been found in the broken columns as shown in Fig. 9(b). 90-degree hooks were found on the loosed hoops. The longitudinal reinforcing bars were obviously too dense and all the lap splices in the column were located on the same section. Fig. 9(c) shows a longitudinal reinforcing bar of the beam not anchored in the core of the column at a failed beam-column joint. The collective result of the structural and construction flaws might have been the cause of the tragic damage that occurred during the earthquake.

(a) Picture after the earthquake (b) Broken column (c) Failed beam-column joint

Fig. 9 – The pictures of Yunmen-Tzueti complex building

3.4.4 Baijin-Shuangxing apartment (Building I) and Wuju-Wusu apartment (Building M)

These two buildings were located on the same street and opposite to each other. Both buildings that collapsed had typical soft-base-floors: the GFs were used as parking spaces and had almost no walls supporting the upper residential floors, which contained lots of partition walls. However, their neighbor building (C) and another residential building (E) both have similar designs and heights but were only subjected to moderate and light damage, respectively. Fig. 3 and Table 3 show that the buildings C and I had similar open GF with similar vertical member ratios. It seems that there should be other factors that aggravated the damage in the buildings I and M. Fig. 10(b) shows one of the few columns that was not buried in the collapsed GF of building I. An inclined breaking line indicating shear failure can be found on the top beam-column joint. Fig. 10(c) magnifies the broken beam end in Fig. 10(b). It appears that there were no proper anchorages or the anchorages that did exist fractured at the ends of longitudinal reinforcing bars in the beam. Building M was reported to be 9-stories high. However, the upper three stories as framed in Fig. 11(a) were illegally added on to the originally 6-story building. Fig. 11(b) shows the strange arrangement of reinforcing bars in the broken column right beneath the add-on at the GF. The picture of the column can be found on Google Street View, as shown in Fig. 11(c). It shows that the column in GF deviated from its position at the upper floors in order to provide sufficient space for parking. The weight of the added three stories might have increased the earthquake inertial force as well as the axial force in the column. Although it is difficult to verify, the GF column might be the first victim of the P-Δ effect due to the deviation and the increased axial force.

(a) Picture after the earthquake (b) Broken column (c) Failed beam-column joint

Fig. 10 – The pictures of Baijin-Shuangxing apartment

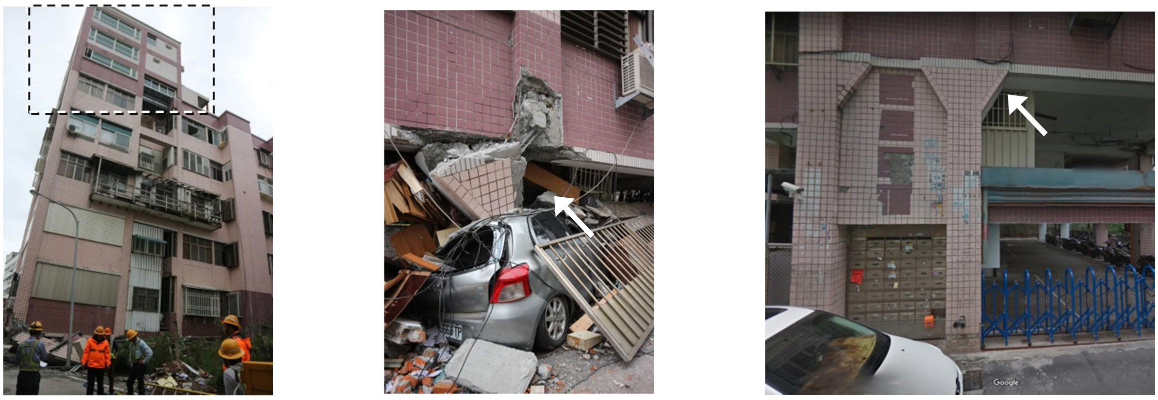

(a) Picture after the earthquake (b) Broken column (c) The broken column before earthquake

Fig. 11 – The pictures of Wuju-Wusu apartment

4. The Effect of Seismic Retrofit

Typical school buildings in Taiwan were found to be vulnerable in past earthquakes. Therefore, The Ministry of Education launched a large-scale seismic retrofit project for the public schools in Taiwan that started in 2008. The school buildings in Hualien City were evaluated and retrofitted because of this project. The authors visited three elementary schools and examined eight school buildings which ranged from 1-story to 4-stories high. Six of the eight buildings were retrofitted using RC shear walls, RC side-walls, and RC column jacketing that were recommended by the National Center for Research on Earthquake Engineering (NCREE). None of the buildings examined had been damaged. Only non-structural damage was found, such as separated expansion joints, dropped ceiling panels and wall tiles, and tilted bookshelves. The result proved the efficiency of the seismic retrofit for low-rise buildings.

5. Conclusions

The 2018 Hualien earthquake had a medium magnitude and the PGAs recorded by most seismic stations were not large. The damage to buildings was not extensive and concentrated on a few buildings. Multiple factors were found to possibly be responsible for the damage to buildings. The severely damaged and collapsed buildings had several common properties. They were all close to the Milun fault, higher than 6 stories, had a fundamental period close to 1.0 s, and had a low vertical member area ratio. Soft/weak-base-floors were found in most of these buildings. Furthermore, particular flaws including non-ductile design, construction defects, and illegal renovations were found in these buildings. These flaws might be the reason why these buildings had more damage than other buildings with similar designs.

The examination of the retrofitted low-rise school buildings found no structural damage and only light damage to non-structural elements. This proved the efficiency of the seismic retrofit methods currently used for low-rise RC buildings in Taiwan.

6. References

[1] NCREE (2018): Reconnaissance report of seismic damages caused by the 6 February 2018 Earthquake, Hualien, Taiwan. *Technical Report NCREE-18-005*, National Center for Research on Earthquake Engineering, Taipei, Taiwan.

[2] Huang MH, Huang HH (2018): The complexity of the 2018 Mw 6.4 Hualien earthquake in east Taiwan. *Geophysical Research Letters*, **45**, 13249-13257.

[3] Lo YC, Yue H, Sun J, Zhao L, Li M (2019): The 2018 M_w6.4 Hualien earthquake: Dynamic slip partitioning reveals the spatial transition from mountain building to subduction. *Earth and Planetary Science Letters*, **524**, 115729.

[4] Central Geological Survey (CGS) (2018). Geology survey report of the 2018.02.06 Hualien earthquake, *Central Geology Survey*, Ministry of Economic Affairs, Taipei, Taiwan.

[5] Yen JY, Lu CH, Dorsey RJ, Chen HK, Chang CP, Wang CC, Chuang RY, Kuo YT, Chiu CY, Chang YH, Bovenga F, Chang WY (2019): Insights into seismogenic deformation during the 2018 Hualien, Taiwan, earthquake sequence from InSAR, GPS, and modeling. *Seismological Research Letters*, **90** (1), 78-87.

[6] Shin TC, Chang CH, Pu HC, Lin HW, Lu PL (2013): The geophysical database management system in Taiwan. *Terrestrial Atmospheric and Oceanic Sciences*, **24**, 11–18.

[7] Kuo CH, Huang JY, Lin CM, Hsu TY, Chao SH, Wen KL (2019): Strong ground motion and pulse-like velocity observations in the near-fault region of the 2018 Mw 6.4 Hualien, Taiwan, Earthquake. *Seismological Research Letters*, **90** (1), 40-50.

[8] Kuo CH, Lin CM, Chang SC, Wen KL, Hsieh HH (2017): Site database for Taiwan strong motion stations, *Technical Report NCREE-17-004*, National Center for Research on Earthquake Engineering, Taipei, Taiwan.

[9] Heaton TH, Hall JF, Wald DJ, Halling MW (1995): Response of high-rise and base-isolated buildings to a hypothetical mw 7.0 blind thrust earthquake. *Science*, **267** (5195), 206-211.

[10] Tu YH, Ao LC, Jean WY (2012): Study on the earthquake damage evaluation procedure for RC and confined masonry buildings. *15th World Conference on Earthquake Engineering (15WCEE)*, No. 0263, Lisbon, Portugal.

[11] Yeh T (2019): Verification of seismic assessment methods using the damaged building data of 2018 Hualien Earthquake. Master thesis, National Cheng Kung University, Tainan, Taiwan.

[12] JBDPA (2001): *Seismic Evaluation and Retrofit for Existing RC buildings*. The Japan Building Disaster Prevention Association.

[13] Lu KW (2001): Investigation in the structure system and earthquake damage of school buildings in Taiwan. Master thesis, National Cheng Kung University, Tainan, Taiwan.

[14] Hwang SJ, Chung LL, Jean WY, Yeh YK, Sher CW, Chang HC, Wang YK, Chen YT (2006): Implementation Planning for Seismic Evaluation and Retrofit of Elementary School Bulidings (II). *Technical Report NCREE-06-004*, National Center for Research on Earthquake Engineering, Taipei, Taiwan.

